Gazi Üniversitesi
Fen Bilimleri Dergisi
PART C: TASARIM VE TEKNOLOJİ

Gazi University
Journal of Science
PART C: DESIGN AND TECHNOLOGY

GU J Sci, Part C, 11(3): 824-836 (2023)

Experimental and Numerical Analysis of an Innovative High Power LEDs Thermal Management System, based on Heat Sink- Heat Pipe Design

Burcu ÇİÇEK[1*] Emre ÜRÜN[2] Necmettin ŞAHİN[1]

[1]*Department of Mechanical Engineering, Aksaray University, 68100, Aksaray, Turkey*

[2]*Department of Institute of Science, Aksaray University, 68100, Aksaray, Turkey*

Article Info

Research article
Received: 15/06/2023
Revision: 22/07/2023
Accepted: 29/07/2023

Keywords

High power LEDs
Heat pipe
Thermal management
Ansys Fluent

Makale Bilgisi

Araştırma makalesi
Başvuru: 15/06/2023
Düzeltme: 22/07/2023
Kabul: 29/07/2023

Anahtar Kelimeler

Yüksek Güçlü LED'ler
Isı borusu
Termal yönetim
Ansys Fluent

Graphical/Tabular Abstract (Grafik Özet)

In this study, two different coolers were designed for LEDs. The study was carried out experimentally and the experimental results were numerically validated using ANSYS Fluent software. / Bu çalışmada LED'ler için iki farklı soğutucu tasarlandı. Çalışma deneysel olarak gerçekleştirildi ve deneysel sonuçlar ANSYS Fluent yazılımı kullanılarak, sayısal olarak doğrulandı.

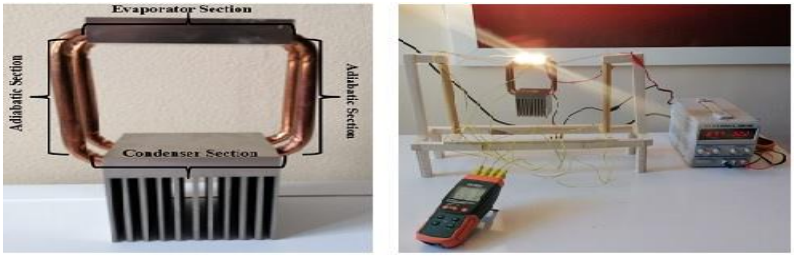

***Figure A**: Heat pipe and experimental set up / **Şekil A:** Isı borusu ve deney düzeneği*

Highlights (Önemli noktalar)

- *Thermal management is of utmost importance in lighting systems in which high-power LEDs are used, especially in small-sized designs. / Yüksek güçlü LED kullanılan aydınlatma sistemlerinde özellikle küçük boyutlu tasarımlarda termal yönetim büyük önem taşımaktadır.*
- *With the increase of LED input power, the luminous flux becomes higher, but also the junction point temperature rises. This situation renders conventional cooling systems insufficient. / LED giriş gücünün artması ile ışık akısı daha yüksek olur ancak bunun yanı sıra birleşme noktası sıcaklığı yükselmektedir. Bu durum klasik soğutma elemanlarının yetersiz kalmasına neden olmaktadır.*
- *Different cooling methods are used for thermal management of LEDs. The heat pipe, which has many advantages over other methods, is widely preferred for the thermal management of LEDs. / LED'lerin termal yönetimi için farklı soğutma yöntemleri kullanılmaktadır. Diğer yöntemlere göre birçok avataja sahip olan ısı borusu, LED'lerin termal yönetimi için yaygın olarak tercih edilmektedir.*

***Aim (Amaç):** In this study, it is aimed minimize the junction temperature of high-power LEDs, especially of the ones used in small spaces. / Bu çalışmada özellikle küçük alanlarda kullanılan yüksek güçlü LED'lerin birleşme noktası sıcaklığını minimum değere düşürmek amaçlanmaktadır.*

***Originality (Özgünlük):** A unique heat sink-heat pipe cooler has been designed and prototypes have been produced for the thermal management of LEDs. / LED'lerin termal yönetimi için özgün bir ısı borusu ve ısı emici kanatçık tasarlanarak prototipler üretilmiştir.*

***Results (Bulgular):** Increasing the LED input power causes an increase in temperature in the entire system. In the system with heat sink-heat pipe, lower junction and solder point temperature values were obtained compared to the other system, which only has a heat sink with fin. / LED giriş gücündeki artış systemin tamamında sıcaklığın artmasına neden olmaktadır. Isı borusu kullanılan sistemde, kanatçıklı soğutma sistemindekine göre daha düşük birleşme noktası ve lehim noktası sıcaklık değerleri elde edilmiştir.*

***Conclusion (Sonuç):** It has been observed that LEDs cooled by HSHP meet the allowable junction temperature limits at all power inputs. However, only heat sink type cooler was insufficient for 100W input power. / Isı borusu ile soğutulan LED'lerin, izin verilen bağlantı sıcaklığı standardını tüm güç girişlerinde karşıladığı gözlenmiştir. Ancak ısı emici kanatçığın kulanıldığı sistemde 100 W giriş gücü için izin verilen bağlantı sıcaklık değeri aşıldığı için yeteriz kalmıştır.*

*Corresponding author, e-mail: burcu_cicek8204@hotmail.com
DOI: 10.29109/gujsc.1315135

GU J Sci, Part C, 11(3): 824-836 (2023)

Gazi Üniversitesi
Fen Bilimleri Dergisi
PART C: TASARIM VE TEKNOLOJİ

Gazi University
Journal of Science
PART C: DESIGN AND TECHNOLOGY

http://dergipark.gov.tr/gujsc

Experimental and Numerical Analysis of an Innovative High Power LEDs Thermal Management System, based on Heat Sink- Heat Pipe Design

Burcu ÇİÇEK[1*] Emre ÜRÜN[2] Necmettin ŞAHİN[1]

[1]*Department of Mechanical Engineering, Aksaray University, 68100, Aksaray, Turkey*

[2]*Department of Institute of Science, Aksaray University, 68100, Aksaray, Turkey*

Article Info

Research article
Received: 15/06/2023
Revision: 22/07/2023
Accepted: 29/07/2023

Keywords

High power LEDs
Heat pipe
Thermal management
Ansys Fluent

Abstract

The efficiency and lifespan of light emitting diodes (LEDs) are adversely affected by junction temperature. Therefore, it is very important to operate the LED at a low junction temperature. In this study, it is aimed to minimize the junction temperature of high power LEDs so that reliability and light output of the device can be maximized.

In the study, a heat pipe heat sink (HPHS) cooler was designed for high power LEDs. The study was carried out experimentally and the results obtained from the experimental study were also verified numerically using the ANSYS Fluent software. Total power inputs ranging between 40 W and 100 W were applied to the LEDs and the performance of the cooler within the current design in those cases was examined. To observe the effect of the heat pipe on the LED junction temperature, a heat sink without heat pipe was also designed and analysed, both experimentally and numerically. The results show that, the heat sink with fin is sufficient at low LED input powers, while at high LED input powers, the HPHS provides much more effective cooling. At the same time, the effect of different thermal interface materials on LED junction temperature was observed, by using materials with thermal conductivities of 1.8, 8.5 and 11 W/m.K for each power input. As the coefficient of thermal conductivity of the thermal interface materials increased, the temperature of the LED solder point decreased.

Isı Emici-Isı Borulu İnovatif Bir Yüksek Güçlü LED Termal Yönetim Sisteminin Deneysel ve Nümerik Analizi

Makale Bilgisi

Araştırma makalesi
Başvuru: 15/06/2023
Düzeltme: 22/07/2023
Kabul: 29/07/2023

Anahtar Kelimeler

Yüksek Güçlü LED'ler
Isı borusu
Termal yönetim
Ansys Fluent

Öz

Işık yayan diyotların (LED'ler) verimliliği ve ömrü bağlantı sıcaklığından olumsuz etkilenir. Bu nedenle, LED'i düşük bağlantı sıcaklığında çalıştırmak çok önemlidir. Bu çalışmada, cihazın güvenilirliğini ve ışık çıkışını maksimize edebilmek için yüksek güçlü LED'lerin bağlantı sıcaklığının en aza indirilmesi amaçlanmaktadır.

Çalışmada, yüksek güçlü LED'ler için bir ısı borulu ısı alıcı (HPHS) soğutucu tasarlanmıştır. Çalışma deneysel olarak gerçekleştirilmiş ve deneysel çalışmadan elde edilen sonuçlar ANSYS Fluent yazılımı kullanılarak sayısal olarak da doğrulanmıştır. LED'lere 40 W ile 100 W arasında değişen toplam güç girdileri uygulanmış ve bu durumlarda soğutucunun mevcut tasarımdaki performansı incelenmiştir. Isı borusunun LED birleşim sıcaklığı üzerindeki etkisini gözlemlemek için, ısı borusu olmayan bir ısı emici de hem deneysel hem de sayısal olarak tasarlanmış ve analiz edilmiştir. Sonuçlar, kanatlı soğutucunun düşük LED giriş güçlerinde yeterli olduğunu, yüksek LED giriş güçlerinde ise HPHS'nin çok daha etkili soğutma sağladığını göstermektedir. Aynı zamanda her güç girişi için 1.8, 8.5 ve 11 W/m.K ısıl iletkenliğe sahip malzemeler kullanılarak farklı termal arayüz malzemelerinin LED bağlantı sıcaklığı üzerindeki etkisi gözlenmiştir. Termal arayüz malzemelerinin termal iletkenlik katsayısı arttıkça LED lehim noktasının sıcaklığı azalmıştır.

*Corresponding author, burcu_cicek8204@hotmail.com
DOI: 10.29109/gujsc.1315135

1. INTRODUCTION (GİRİŞ)

In recent years, light emitting diodes (LEDs) are becoming increasingly popular lighting sources, as a result of commercial applications and research. This is due to the advantages of LEDs such as low energy consumption, high optical efficiency, long lifespan and good controllability.

LEDs are semiconductor devices and, unlike traditional lighting, generally do not use glass and filaments [1-3]. Also, LEDs do not contain mercury like fluorescent lamps do. While the luminous efficiency of LEDs is much superior to that of incandescent lamps, it is also comparable to that of fluorescent lamps [4-9]. Today, LEDs are rapidly replacing fluorescent lamps. Like standard diodes, LEDs consist of p-type and n-type semiconductor materials that form a p-n junction.

Although usage of LEDs in lighting is not new, gradual development of LED technology and introduction of more innovative solutions make LEDs increasingly indispensable [10]. In the near future, it is thought that LEDs will replace other lighting technologies and will be effective in many fields such as clinical medicine, general lighting, industrial lighting and street lighting.

With the recent advances in technology, sizes of LEDs, like other semiconductor devices, are shrinking. This naturally causes an increase in heat dissipation, heat flux and power. When a LED is powered, the luminescence reaction takes place at the p-n point and the energy is converted into light. However, as the luminescence reaction goes on, only part of the energy is converted into luminous flux, the rest dissipates in the form of heat. During the heat generation, the joint on the device is the highest temperature point within the device. The temperature at this point is referred as the junction temperature. The junction temperature of a LED is vital because lifespan and luminous flux are dependent on it.

If the heat generated in a LED is not properly dissipated, this will cause an increase in the junction temperature of the bulb. If the temperature gets excessively high, optical and energy efficiencies and bulb life are considerably reduced [11]. Therefore, effective thermal management is strongly needed, in the operation of high power LEDs. Thanks to thermal management, failure risk is reduced and it is ensured that the LEDs operate safer and provide better light quality. Many methods are used for thermal management of LEDs. For example, natural convection heat sinks are widely used to cool LED packages. Heat sinks do not consume additional energy and do not expose the system to acoustic and overload problems. The purpose of adding a heat sink to LED systems is to allow heat transfer to the ambient environment for keeping the junction at a lower temperature. In [12-14], heat transfer by natural convection with the aid of heat sinks were investigated both numerically and experimentally. There are also a number of recent studies aiming to control heat dissipation using heat sinks.

Studies have shown that effective thermal management of LEDs is strongly dependent upon the fin structure, fin geometry and also the materials placed under the heat sinks [15-16]. The thermal interface material, whose function is reduction of the thermal resistance between the LED and the heat sink, is very important in transmitting the excess heat in the LED. Tang et al. [17] numerically investigated the variation of the thermal resistance with respect to thermal interface materials. In another study by Abdelmlek et al. [18], insufficient thermal interfacial material was improved.

In recent years, usage of heat pipes, especially for effective heat dissipation in high-power LEDs, is also very common due to their very high coefficient of thermal conductivity. Moon et al. [19] used a U-shaped straight aluminum heat pipe to remove heat from a 100W COB LED lamp. They investigated the heat transfer properties of the heat pipe with two condensers. Sosoi et al. [20] designed a cylindrical heat pipe to cool high-power LEDs and numerically analyzed it for certain conditions. They assessed the resulting junction temperatures. Joshi et al. [21], numerically investigated a model to simulate the slurry flow and the solid particulate matter transportation, which are varied by flow parameters. Çiftçi [22], investigated thermal effects of nanofluids on heat pipe experimentally.

Huang et al. [23] designed a grooved heat pipe fin for high power LEDs used in the automotive industry. They analyzed their system in ANSYS software with different heat sinks and printed circuit board materials, as well as different fin geometries. Wang et al. [24] fabricated a tubular oscillating heat pipe formed with sintered copper particles in a flat plate evaporator for thermal management of high power LEDs. The thermal performance of the oscillating heat pipe and the light and temperature distribution of the LED array have been experimentally tested and calculated. The thermal resistance obtained 0.168 W/m.K and the maximum LED temperature was below 70 °C for 60 W LED input power. Lu et al. [25] designed a heat pipe-

heatsink system for the high-power LED package. The thermal resistance of the LED package has been tested experimentally. Tang et al. [26] experimentally investigated an active cooling system with heat sink-heat pipe for high-power automobile LED lighting.

In our study, a heat pipe heat sink (HPHS) is designed for cooling high power LEDs. The system is designed in such a way that four C-shaped copper heat pipes are integrated into the evaporator and condenser area of the aluminum heat sink. The system is manufactured according to the design and four high-power COB LEDs are mounted on top of the upper heat sink to dissipate the generated heat. The aim of the study is to keep the junction temperature of high power LEDs below the specified limit. This is because if the junction temperature exceeds this limit, which can happen at high powers, the optical efficiency and operational life of the LED begin to deteriorate. In the study, different power values from 40 W to 100 W in total were applied to the high-power LEDs and temperature values were measured at certain points until the system reaches the steady-state. By using the parameters such as measured temperature values and LED input powers, the junction temperature, which is important for the LEDs thermal performance, has been calculated. In addition, the effect of coefficient of thermal conductivity of the thermal interface materials, which were placed between the LEDs and the heat sink, are evaluated.

Today, both technological developments and architectural concerns favour smaller sized designs in electronic devices. In this context, it is thought that the current study will provide an innovative solution for thermal management in lighting applications, especially in restricted spaces where high luminous flux is required.

2. MATERIALS AND METHODS (MATERYAL VE METOD)

The study consists of two parts including thermal analysis of the heat sink-heat pipe cooler and the heat sink without heat pipe cooler. In the first part, the designed cooler models were manufactured and experimental measurements were carried out. In the second part, the thermal behavior of the designed cooler models has been simulated in Ansys.

2.1. Experimental Study (Deneysel Çalışma)

In this study, two different designs were used and their cooling performances were tested for high power LEDs. In the first design, four identical C-shaped copper heat pipes were used. A screen mesh wick structure is utilized to provide capillary effect and thermal conductivity inside the heat pipes. Distilled water was selected as the working fluid. The characteristics of the heat pipe used in the study are listed in Table 1.

Table 1. Heat pipe specifications (All lengths in mm) (Isı borusu özellikleri)

Length of the heat pipe	229
Length of the evaporation zone	62
Length of the adiabatic zone	105
Length of the condensation zone	62
Outer diameter of the heat pipe	8
Inlet diameter of the heat pipe	7.25
Working fluid	Water
Wick type	Screen Mesh
Mesh size	200 Mesh/in

In the first design, the LEDs were located on the top of the heat sink which houses the evaporator zone of heat pipe (figure 1). Fins were also added on the bottom of the heat sink which houses the condenser of the heat pipe to increase heat transfer.

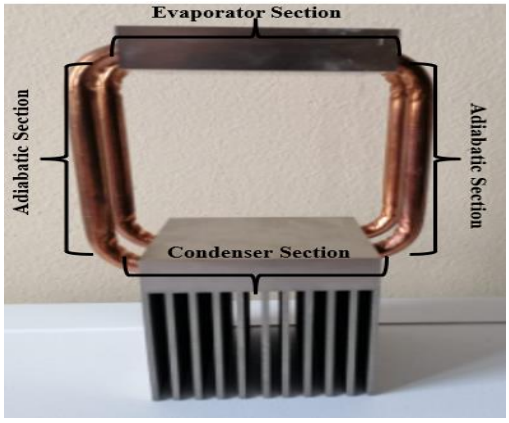

Figure 1. Heat sink-heat pipe system for cooler (Soğutma için ısı emici-ısı borulu sistem)

In the second design, the LEDs are mounted on top of the heat sinks without heat pipe as seen in figure 2. Aluminum fins were installed at the heat sink's bottom side.

Figure 2. Heat sink with fins for cooler (Soğutma için kanatçıklı ısı emici)

COB LEDs were used in the study. The LEDs were soldered so that the COB LEDs could be electrically powered. TT-TECNIC RXN 605D model adjustable power supply, which provides power up to 60 volts voltage and 5 ampere current, was used to feed the LEDs with parallel electrical connections.

Four K type thermocouples were used for temperature measurements. Thermocouples were connected to the Extech SDL200 datalogger to record the temperature measurement values at specific time intervals. Starting from the application of electrical power to the LEDs, measurements were taken until thermal equilibrium was established. During the experiment, the ambient temperature and the air speed were measured as 24.5 ± 0.3 °C and 0.1 m/s, respectively. In Figure 3, the experimental setup is depicted.

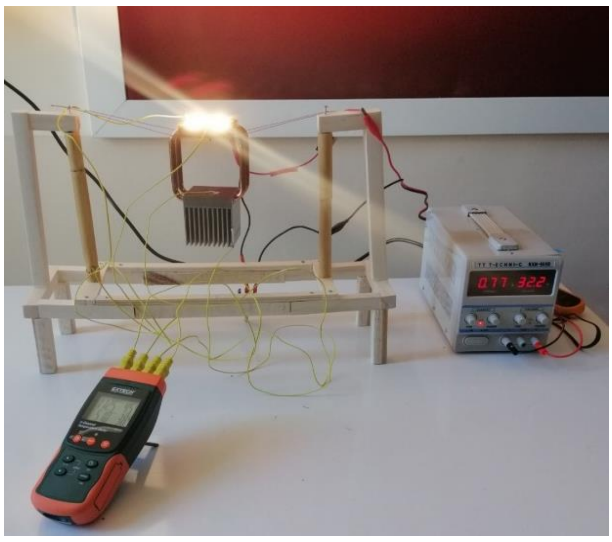

Figure 3. View of experimental set up (Deneysel kurulumun görünümü)

Experimental uncertainty (Deneysel belirsizlik)

Experimental uncertainty is basically defined as the random error in a measurement. Uncertainties are thought to be due to the variations in electrical power input and errors in instrument calibrations. In uncertainty analysis, the approach proposed by Kline[27] and a root of sum of squares (RSS) method based approach [28] has been taken.The thermocouples can measure the temperature within a ± 0.1 °C error range. Therefore absolute uncertainty related to the temperature measurement, dT, is taken as 0.1 °C. The error in the voltage measurement(dU), the error in the current measurement(dI) and the SD card resolution (dT,data) were taken as, ± 0.5 Volt, ± 0.5 Ampere and ± 0.1 °C, from the respective devşce specification. The total uncertainty related to the temperature measurement (U_T) is expressed as equation (1), taking all uncertainties. Here, T_{ave} indicates the average value at each temperature measuring point. As a result of the calculations, it was seen that the uncertainty value changed between 1.3% and 2.4%.

$$U_T = \sqrt{(\frac{dT}{T_{ave}})^2 + (\frac{dT_{data}}{T_{ave}})^2 + (\frac{dU}{U})^2 + (\frac{dI}{I})^2} \quad (1)$$

U_T: Total uncertainty related to the temperature measurement

dT: Absolute uncertainty related to the temperature measurement

dU: Uncertainty related to the voltage measurement

dI: Uncertainty related to the current measurement

dT_{data}: SD card resolution

T_{ave}: Average temperature

2.2. Numerical Solution (Nümerik Çözüm)

Geometry and mesh structure (Geometri ve mesh yapısı)

Model files are formed using Design Modeling of ANSYS 19.1 The simulation was done using ANSYS Fluent package. For meshing, The Patch Conforming Method was used. In this method, a dedicated tetrahedral mesh is created. Compared to other sub-methods of The Patch Comforming method, such as Multizone, Hexagonal Dominant and Sweep, it has been observed that tetrahedral

meshing captures the curvatures more accurately [29]. The Patch Conforming Method enables the meshing to be refined when needed and allows fast computation while preserving larger cells. The mesh creation process starts from the edges, then it continues from the surfaces and towards to volumes in the end. All surfaces and boundaries are matched to each other and this allows for high quality mesh structures. While creating the mesh structure, some quality parameters are required to be in the desired range. The shape of the cell is important for accurate analysis. Accordingly, in order to create a high quality mesh, the Skewness value, which is defined as the difference between the shape of the cell and the shape of an equilateral cell with an equivalent volume, is desired to be lower than 0.96 and the Aspect Ratio, which is the ratio of the minimum element edge length to the maximum element edge length, is also desired to be less than 100 [30]. In addition, the mesh orthogonal quality value also gives important clues about the mesh quality. Orthogonal quality ranges from 0 to 1. Orthogonal quality values closer to 1 indicate higher quality mesh structures. The mesh quality parameter values obtained for both designs are given in Table 2.

In order to get the most accurate mesh element number, the mesh independence study was performed. In Figure 4, the LED solder point temperatures with respect to the mesh structure, which was created by using different element sizes for both designs, are plotted.

Table 2. Mesh quality parameters (Mesh kalite parametreleri)

Mesh	First Model	Second Model
Element numbers	1346081	953461
Nodes numbers	255343	172556
Aspect ratio, min	1.05	1.16
Aspect Ratio,max	14.43	15.08
Skewness, max	0.89	0.85
Orthogonal quality, ave	0.74	0.75

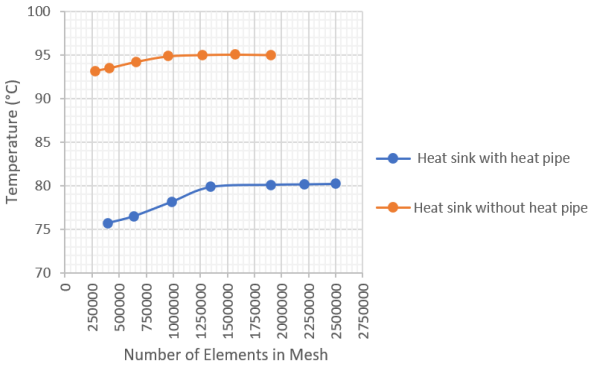

Figure 4. Mesh indepence study for both designs (Her iki tasarım için mesh bağımsızlık çalışması)

Accordingly, the optimal mesh element numbers were found as 1346081 and 953461 for the first and the second design, respectively. In figure 5 and figure 6, mesh structures of both designs are depicted.

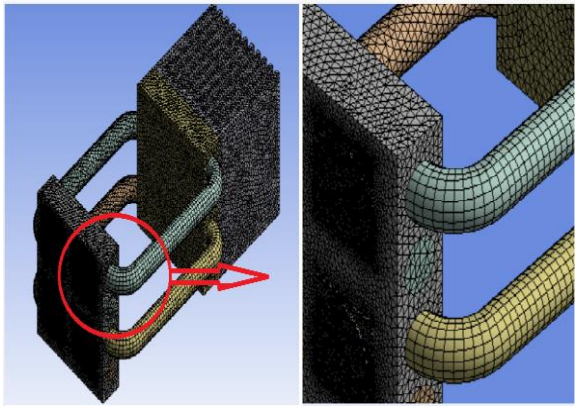

Figure 5. Mesh structure of HPHS with fins (Kanatçıklı HPHS'nin mesh yapısı)

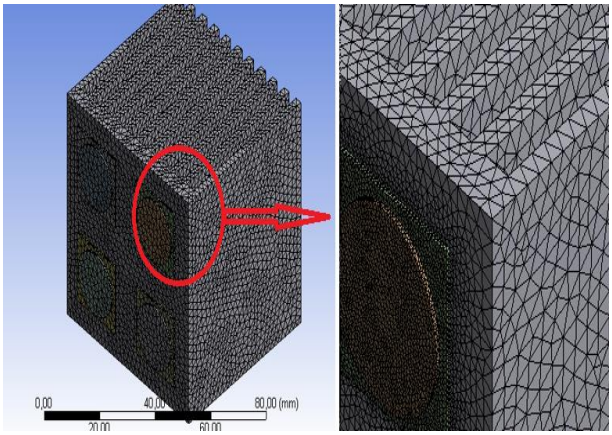

Figure 6. Mesh structure of heat sink with fins (Kanatçıklı ısı emicinin mesh yapısı)

Solution method and technique (Çözüm metodu ve tekniği)

Using Computational Fluid Dynamics (CFD) analysis, experimental results can be verified The simulation is used to transform the Navier-Stokes equations into difference equations and obtain

solutions based on numerical analysis techniques. In the study, ANSYS Fluent 19.1 software was used to conduct numerical analyzes under different conditions. In order to compare experimental results with the simulation results, the following assumptions were made:

- All phase changes took place in incompressible flow.
- The steam flow created a turbulence.
- Except for heating and cooling, the heat pipe was adiabatic.

Governing equations (Korunum denklemleri)

In the heat pipe, Governing Equations including the energy, mass and momentum equations are solved in ANSYS Fluent to describe the fluid's motion during the evaporation and condensation process. The VOF (Volume of Fluid) method is used for interface calculations. In multiphase flows, adjacent phases do not have static interfaces. This means, in the phase interfaces, physical properties, e.g. viscosity, exhibit a variation. These facts cause a heavy computational workload. Therefore, numerical solutions based on the finite volume method are harder to perform for multiphase flows than they are for single phase flows. In the VOF technique, a solution is reached by defining the movement of all the phases and interfaces. In order to track the motion of each phase, the VOF model defines their volume fractions and makes use of a Navier-Stokes equation set.

Conservation equation formulas are given below.

Conservation of Mass:

$$\frac{\partial(\mathrm{qu})}{\partial \mathrm{x}}+\frac{\partial(\mathrm{qv})}{\partial \mathrm{y}}+\frac{\partial(\mathrm{qw})}{\partial \mathrm{z}}=0 \qquad (2)$$

Conservation of Momentum:

$$\frac{\partial(\mathrm{qu}^2)}{\partial \mathrm{x}}+\frac{\partial(\mathrm{quv})}{\partial \mathrm{y}}+\frac{\partial(\mathrm{quw})}{\partial \mathrm{z}} = -\frac{\partial \mathrm{P}}{\partial \mathrm{x}} + \mu\left(\frac{\partial^2 \mathrm{u}}{\partial \mathrm{x}^2}+\frac{\partial^2 \mathrm{u}}{\partial \mathrm{y}^2}+\frac{\partial^2 \mathrm{u}}{\partial \mathrm{z}^2}\right) \qquad (3)$$

$$\frac{\partial(\mathrm{quv})}{\partial \mathrm{x}}+\frac{\partial(\mathrm{qv}^2)}{\partial \mathrm{y}}+\frac{\partial(\mathrm{qvw})}{\partial \mathrm{z}} = -\frac{\partial \mathrm{P}}{\partial \mathrm{y}} + \mu\left(\frac{\partial^2 \mathrm{v}}{\partial \mathrm{x}^2}+\frac{\partial^2 \mathrm{v}}{\partial \mathrm{y}^2}+\frac{\partial^2 \mathrm{v}}{\partial \mathrm{z}^2}\right) \qquad (4)$$

$$\frac{\partial(\mathrm{quw})}{\partial \mathrm{x}}+\frac{\partial(\mathrm{qvw})}{\partial \mathrm{y}}+\frac{\partial(\mathrm{qw}^2)}{\partial \mathrm{z}} = -\frac{\partial \mathrm{P}}{\partial \mathrm{z}} + \mu\left(\frac{\partial^2 \mathrm{w}}{\partial \mathrm{x}^2}+\frac{\partial^2 \mathrm{w}}{\partial \mathrm{y}^2}+\frac{\partial^2 \mathrm{w}}{\partial \mathrm{z}^2}\right) + \mathrm{g}(\mathrm{q} - \mathrm{q}_0) \qquad (5)$$

Conservation of Energy:

$$\frac{\partial(\mathrm{quT})}{\partial \mathrm{x}}+\frac{\partial(\mathrm{qvT})}{\partial \mathrm{y}}+\frac{\partial(\mathrm{qwT})}{\partial \mathrm{z}} = \frac{\mathrm{k}}{\mathrm{C_p}}\left(\frac{\partial^2 \mathrm{T}}{\partial \mathrm{x}^2}+\frac{\partial^2 \mathrm{T}}{\partial \mathrm{y}^2}+\frac{\partial^2 \mathrm{T}}{\partial \mathrm{z}^2}\right) \qquad (6)$$

Convergence criteria (Yakınsama kriteri)

The VOF model depends on whether each cell in the field is used by one phase or two phases combined. Ansys Fluent is not capable of simulating phase changing materials when they undergo evaporation or condensation.

Evaporation, condensation and phase changes in the heat pipe are considered by utilizing User Defined Functions (UDF) in Fluent software. UDF is required especially for necessary calculations of mass and heat transfer between vapor and liquid phases, as naturally occuring during the condensation and evaporation. The model makes the calculations by using energy and continuity equations. For this purpose, the source terms in the governing equations are used. Mass and Energy terms are defined in the UDF and associated with conservation equations in Fluent. The volume fraction of each phase in the cells was defined by the VOF model. There are three possible conditions in the VOF model:

$\alpha_L = 1$, The entire of heat pipe is in liquid phase

$\alpha_L = 0$, The entire of heat pipe is in vapor phase

$0 < \alpha_L < 1$,

The fluid in the heat pipe is between liquid and vapor phase [31].

In the evaporation process, in order to calculate the mass transfer, two mass terms are required: the mass added to the vapor phase and the mass subtracted from the liquid phase. The converse applies for the condensation process. The equations defining vapor-to-liquid mass transfer are listed in Table 3. Source terms were derived by De Schepper et al. [32] to be incorporated into the governing equations used by the VOF model in Fluent Ansys.

Table 3. Source term for vapor-to-liquid mass transfer[32] (Buhardan sıvıya kütlesel geçiş için kaynak terimi)

Evaporation	
Liquid phase	$S_M = -0.1\alpha_l\rho_l\frac{T_l - T_{sat}}{T_{sat}}$
Vapor phase	$S_M = 0.1\alpha_l\rho_l\frac{T_l - T_{sat}}{T_{sat}}$
Condensation	
Liquid phase	$S_M = 0.1\alpha_v\rho_v\frac{T_l - T_{sat}}{T_{sat}}$
Vapor phase	$S_M = -0.1\alpha_v\rho_v\frac{T_l - T_{sat}}{T_{sat}}$

In the heat transfer, a single source term is sufficient for both phases. It is obtained by multiplying the mass source terms by the latent heat. Source terms for heat transfer are given in Table 4.

Table 4. Source term for the energy transfer from vapor to liquid phase[32] (Buhardan sıvıya enerji geçişi için kaynak terimi)

Evaporation	$S_E = -0.1\alpha_l\rho_l\frac{T_l - T_{sat}}{T_{sat}}\Delta H$
Condensation	$S_E = 0.1\alpha_v\rho_v\frac{T_l - T_{sat}}{T_{sat}}\Delta H$

S_M: Mass source term

S_E: Energy source term

ρ_l: Liquid density

ρ_v: Vapour density

T_l: Liquid temperature

T_{sat}: Saturation temperature

ΔH: Enthalpy difference

α_l: Liquid phase ratio

α_v: Vapor phase ratio

A steady-state model of the dynamic behavior of the two-phase flow and the heat transfer from the fins by natural convection has been developed. For the VOF model, the maximum number of Courants used near the interface is taken as 200, as advised in [31]. In the simulation, the "Second Order Upwind Scheme" was used to solve the energy and momentum equations and the "SIMPLE Algorithm" was selected for modelling the relation between the pressure and the velocity. When the "scale residual" for the energy and mass components reached 10^{-5}, it is assumed that the convergence criterion is satisfied.

In the study, water vapor was defined as the first phase and liquid water was defined as the second phase. For the heat and mass transfer calculations during the vaporisation and liquefaction processes, the boiling point and the latent heat of evaporation values were entered (as UDF code) as 373 K and 2260 kJ/kg, respectively.

Boundary conditions (Sınır koşulları)

The operating pressure is set to 400,000 Pa with a surface tension coefficient of 0.070 for the phase interaction. The phase change propagated along the direction of the heat pipe with a velocity of 0.01 m/s. Natural convection assumptions are applied for heat transfer on the cooler side. The heat transfer coefficient of the air in the cooler side is taken as 10 W/m.K. The heat transfer coefficient (h) is assumed to be zero in other parts of the system. Natural convection assumptions also apply for heat transfer on the heat sink.

3. RESULTS AND DISCUSSION (SONUÇLAR VE TARTIŞMA)

In the experimental study, temperature measurements were done at certain points for determining the cooling performance of the HPHS system. In order to determine the thermal performance of the HPHS, total power values of 40, 60, 80 and 100 W were applied to the LEDs mounted on it.

The measurements continued until the system reached thermal equilibrium, for each input power. Data were recorded in the data logger at intervals of 2 s for approximately one hour. The measurement values for 100 W LED input power are given in Figure 7. Here, T1 is the solder point temperature of the LED chip, T2 is the bottom surface temperature of the heat sink where the heat pipe evaporator is located, T3 is the bottom surface temperature of the heat sink where the heat pipe condenser is located and T4 is the fin tip temperature. According to this chart, temperature increases were observed at each measurement point, after the application of thermal power to the LEDs. Since the LED solder point is the closest point to the heat source, the temperature increase on LED solder point was quicker than the increase at other measurement points. Heat, in later times, with the effect of the heat pipe, started to be transferred from the LED to the fin. It was observed that, at T2, T3 and T4 points, the temperature first increased up to a certain value and then it was stabilized. Similar pattern in time-dependent temperature distribution was also observed in the tests with different input powers to the LED.

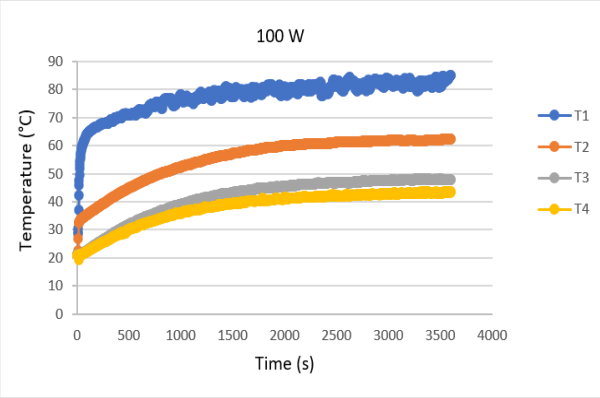

Figure 7. Time dependent temperature value at certain points for 100 W LED input power (100 W'lık LED giriş gücü için belirli noktaların zamana bağlı sıcaklı değerleri)

In Figure 8, the final results at the four measurement points above the heat pipe- heat sink are given for different LED input powers. According to this chart, it is seen that the temperature difference in the heat pipe increases as the power given to the LEDs increases. LED solder point temperatures were measured as 60.8, 68.4, 75.2 and 83.8 °C for LED input powers of 40, 60, 80 and 100 W, respectively.

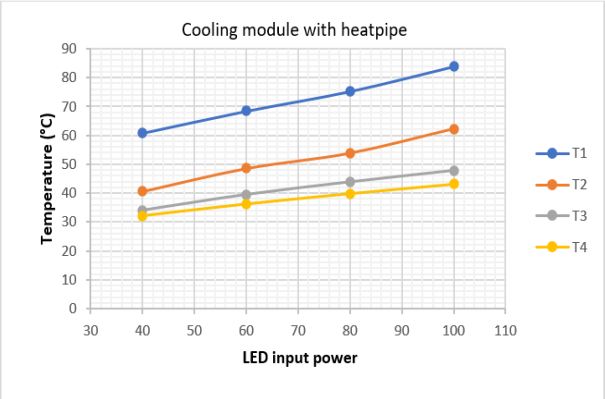

Figure 8. Temperature values at certain points for different LED input power (Farklı LED giriş güçleri için belirli noktalardaki sıcaklık değerleri)

ANSYS 19.1 software was used for verification of experimentally measured temperature values. The HPHS design was drawn in ANSYS Workbench and simulated in ANSYS Fluent with the same boundary and initial conditions as the experimental system. In Figure 9, charts provided by the software, depicting the temperature distribution for each input power, are given.

It was seen that the results obtained from the numerical simulation and experimental study were compatible with each other, and there was a small relative difference of about 0.994% between the measured and simulated temperature values. The difference was calculated by R2 squared regression in Excel. It was seen that the results obtained from the numerical simulation and experimental study were compatible with each other, with a coefficient of determination (R^2) value of 0.994

LED solder point temperature (T1), is critical in calculating the junction temperature. In Figure 10, the solder point temperatures obtained in the experimental (T1) and numerical (T1') studies are given, for various LED input powers. As seen in the chart, while the soldering point temperature was approximately 60° C at 40 W LED input power, this value increased to 67, 74 and 82° C at 60, 80 and 100 W, respectively.

When comparing the temperature values at the soldering point obtained in the experimental and numerical studies, it is seen that the maximum difference between the two was 3.6 °C. The difference is calculated as 2.5, 2.7 and 3.6 °C for 60, 80 and 100 W LED input powers, respectively. It is clear that the soldering point temperature values obtained in both methods are very close to each other.

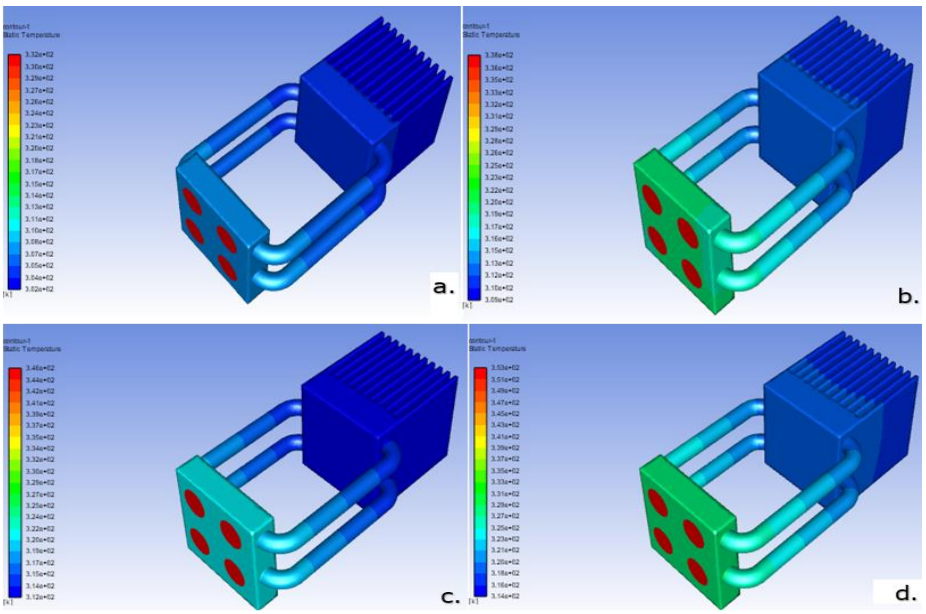

Figure 9. Temperature distributions for a. 40 W LED input power, b. 60 W LED input power, c. 80 W LED input power, d. 100 W LED input power (a. 40 W LED giriş gücü için, b. 60 W LED giriş gücü için, 80 W LED giriş gücü için, 100 W LED giriş gücü için sıcaklık dağılımı)

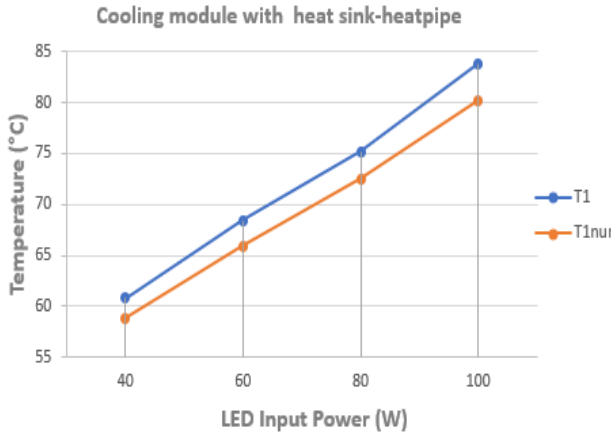

Figure 10. Soldering point temperatures for different LED input powers in experimental and numerical study (Deneysel ve sayısal çalışmadaki farklı LED giriş güçleri için lehimleme noktası sıcaklığı)

In order to see the effect of the heat pipe on the cooling performance in the HPHS, only an heat sink with fin design was also manufactured as a second design. The second design was tested experimentally and numerically with the same boundary conditions and the same LED input powers. In Figure 11, temperature values obtained from the experimental study of the second design, for 40, 60, 80 and 100 W LED input powers, at certain measuring points are given. LED solder point temperatures were measured as 65.5, 76.3, 87.4 and 98.2°C for LED input powers of 40, 60, 80 and 100 W, respectively.

In the chart, T1' is the LED solder point temperature, T2' is the Electronic Circuit Board temperature, T3' and T4' are the temperatures at the bottom and top points of the fin structure, respectively.

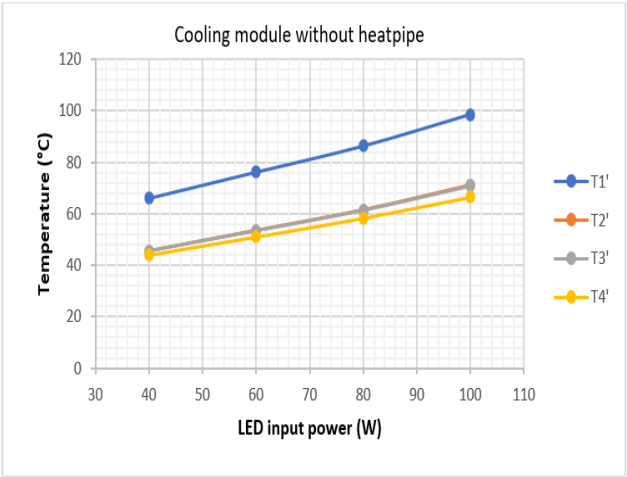

Figure 11. Temperature value of certain points for different LED input power (Farklı LED giriş güçleri için belirli noktalardaki sıcaklık değeri)

In Figure 12, the temperature distribution obtained from the simulation at different LED input powers for the secondary design is given. LED solder point temperatures were calculated as 58.8, 65.9, 71 and 95.2 °C for 40, 60, 80 and 100 W LED input powers, respectively. It is seen that the results obtained from the experimental and numerical modeling for the second design are compatible with one of them. The

coefficient of determination(R^2) was calculated as 0.998, very similar to the first design.

In figure 13, the solder point temperatures obtained in experimental (T1) and numerical (T1') studies are given. for various LED input powers on the second design. As seen in the chart, while the soldering point temperature was approximately 65° C at 40 W LED input power, this value increased to 75, 85 and 96° C at 60, 80 and 100 W, respectively. When comparing the temperature values at the soldering point obtained in the experimental and numerical studies, it is seen that the maximum difference between the two was 2.3 °C. This value is determined as 2.3, 2.6 and 3.2 °C for 60, 80 and 100 W LED input powers, respectively.

One of the most important parameters defining the thermal performance of LEDs is the junction temperature. The junction temperature cannot be measured directly and can be determined by the following equation [33].

$$T_j = T_s + P * R_{j-s} \quad (7)$$

T_j: Junction tempeature

T_s: Soldering point temperature

$R_{j\text{-}s}$: Thermal resistance from the LED junction point to the soldering point

P: LED input power

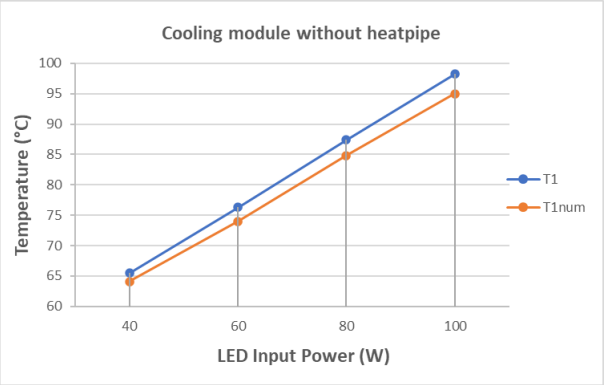

Figure 13. Soldering point temperatures for different LED input powers in experimental and numerical study (Deneysel ve sayısal çalışmadaki farklı LED giriş güçleri için lehimleme noktası sıcaklığı)

Here T_{j-s} is the soldering point temperature, R_{j-s} is the thermal resistance from the LED junction point to the soldering point. The latter value is usually provided in the datasheet of the LEDs. The R_{j-s} value of the Lumileds Luxeon 1208 model COB LED used in this study was read from the datasheet as 0.29 W/°C [34]. The T_s value can be taken into account by measuring it directly. P stands for LED power.

Junction temperature values are calculated by using the measured temperature values and the different power values of 40, 60, 80 and 100 W of the LEDs both designs. The allowable limit for junction temperature is 120 °C for the COB LEDs used. When the chart in figure 14 is examined, the junction temperature of LEDs cooled by HPHS is seen to stay below the allowable limit even for 100W input power. For the same input power, the LED junction temperature of the LEDs cooled by heat sink with fin only is calculated as approximately 125°C. This value is above the allowable junction temperature limit. In other words, it has been observed that, heat sink with fin alone cannot provide sufficient cooling. For all the other power inputs of the LED, the junction temperature of the LEDs used with the HPHS is lower than those of heat sink with fin. It may be thought that keeping the junction temperature below the maximum allowable limit suffices but indeed every reduction in it translates into longer LED lifespan and better optical efficiency. Therefore, it is recommended to use the first design, especially at high input powers.

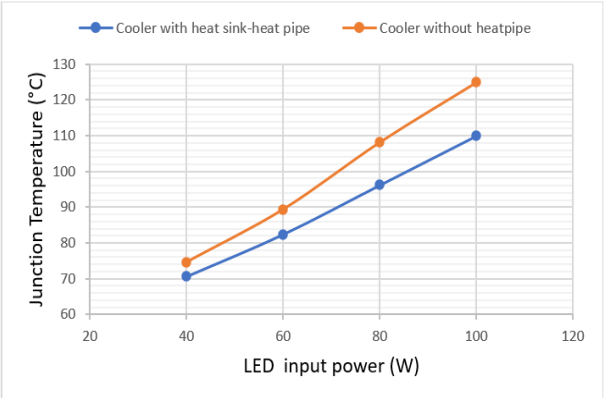

Figure 14. Junction temperature for different LED input power (Farklı LED giriş güçleri için jonksiyon sıcaklıkları)

When we compare this study to the existing literature, we observe that it has a significant novelty value. For example, Zhang et al. [35] used a copper based plate with an aluminum radiator, which is of larger size than our designs. Their design managed to cool the copper base of the LED under 100 W heat power load down only to 100.5 C. In another study, Lu et al. [36] improved a loop heat pipe for thermal management of high power LED's. The maximum temperature of the heat pipe didn't exceed 100 °C for 100 W LED heat load.

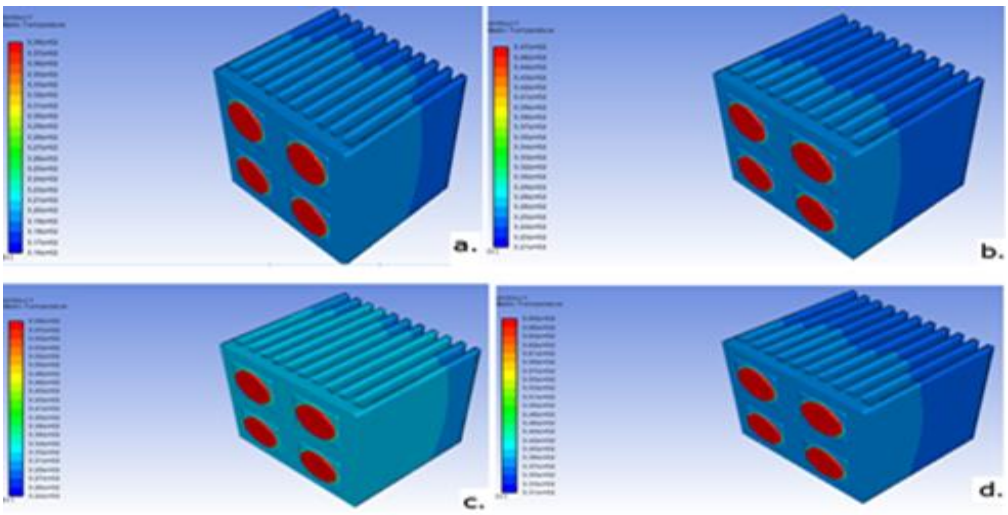

Figure 12. Temperature distubitions for a. 40 W LED input power, b. 60 W LED input power, c. 80 W LED input power, d. 100 W LED input power (a. 40 W LED giriş gücü için, b. 60 W LED giriş gücü için, 80 W LED giriş gücü için, 100 W LED giriş gücü için sıcaklık dağılımı)

In electronic cooling, air gaps between the heat generating electronic components and the heat sink adversely affect the heat transfer from the electronic component to the heat sink. In order to reduce the additional thermal resistance created by the interface between the LED and the heat sink, a thermal interface material is used. Thermal interface materials consist of thermally conductive polymer or silicon matrix particles [37]. In this study, thermal interface material with a thermal conductivity of 11 W/m.K was used in both designs. The resulting temperature values are given in Figure 15. In addition, thermal interface materials with thermal conductivities of 1.5 and 8.5 W/m.K, were used for the heat pipe -heat sink with a total LED power of 100 W and their effects on cooling performance were compared.

According to the measurements, the temperature at the solder point, which is the closest measurement point to the LED junction point, varies inversely with the thermal paste's coefficient of thermal conductivity. When a thermal paste with a thermal conductivity coefficient of 1.8 W/m.K was used, T1 soldering point temperature was measured as 106.4 °C under 100W LED input power. When thermal paste is replaced with a one that has a thermal conductivity coefficient of 8.5 W/m.K and 11 W/m.K were used, it declined to 87.9 and 83.8 °C, respectively.

a.

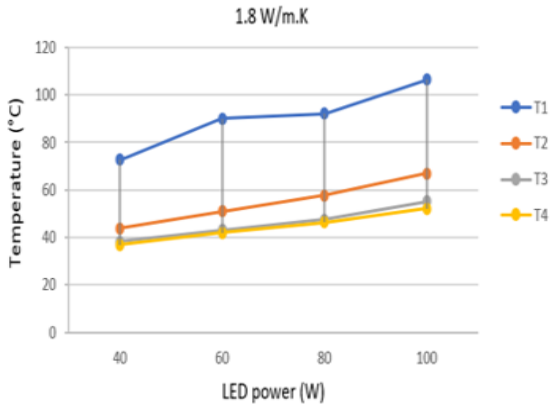

b.

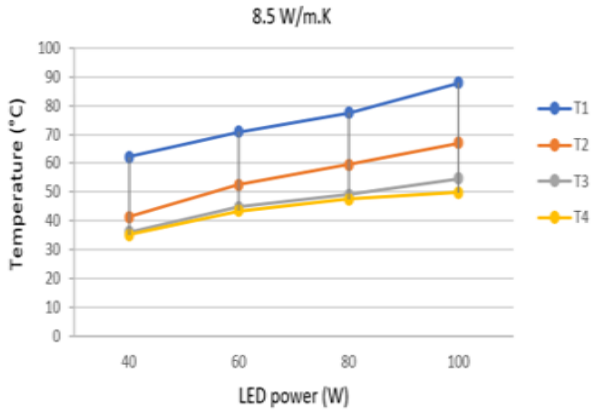

Figure 15. a, For 1.8 W/m.K and b, for 8.5 W/m.K heat conduction coefficient of thermal paste, variation of temperature at measurement points for different LED power inputs (Isı taşınım katsayısı a. 1.8 W/m.K ve b. 8.5 W/m.K olan temal macunlar için farklı LED giriş güçlerinde ölçüm noktalarının sıcaklık değişimi)

4. CONCLUSIONS (SONUÇLAR)

In this study, a HPHS acting as a passive cooler for light emitting diodes (LEDs) was designed, manufactured and experimentally tested. The results of the experimental study was also verified by numerical analysis in the ANSYS Fluent software. The heat pipe is particularly advantageous for high-power microelectronic systems, as it has no moving parts, no additional energy input requirement, a low maintenance cost and a high thermal conductivity. In the cooling of micro-sized but high-power LEDs, it is cruical that the cooler is compact in size, especially in the areas where the architectural structure is the primary focus and thus the space is restricted. Compactness will also help keeping the material costs low. For a better understanding of the thermal effect of the heat pipe, its performance was compared to the performance of a heat sink with fins type of cooler. The heat dissipation capabilities of both designs were investigated for various LED power inputs. Here are the conclusions that can be drawn:

- It has been observed that LEDs cooled by heat pipe- heat sink type cooler met the allowable junction temperature standard at all power inputs, but the heat sink with fin exceeds the allowable junction temperature value at 100 W input power and is not sufficient at such high power inputs.

- While the differences between the LED junction temperatures of the designs were as low as 4 °C at a lower power input such as 40 W, it increased to 7, 12 and 15 °C, respectively, at the 60, 80 and 100 W power inputs.

- It can be said that the design with a heat sink with fins type cooler is a better option at lower power inputs, because it can satisfy the criteria at a lower cost, whereas the design with HPHS type of cooler is the better option at high powers because it becomes the only option that satisfies the criteria.

- The effect of thermal pastes with different heat transfer coefficients used on the interfaces between LED and heat sink on the LED junction temperature was investigated. When thermal paste with 11 W/mk heat transfer coefficient was used instead of 1.8 w/m.k thermal paste a decrease of approximately 22.6 °C in the junction temperature was observed. This showed the importance of the thermal conductivity coefficient of the thermal interface material.

- The junction temperature was calculated as 110 °C for 100W LED input power for the first design (heat sink heat pipe). Since this value is below the LED junction temperature limit, the design is considered to provide sufficient cooling.

- The junction temperature was calculated as 125 °C for 100W LED input power for the second design (heat sink without heat pipe). This value exceeds the LED junction temperature limit. Therefore, it can be said that the cooling capacity of the second design is not sufficient for 100W LED input power.

ACKNOWLEDGMENTS (TEŞEKKÜR)

The present work was financially supported by Aksaray University Scientific Research Coordinator under Research Project, number of Project: 2021-30./ Çalışma Aksaray Üniversitesi BAP birimi 2021-30 nolu projesi tarafından desteklenmiştir.

DECLARATION OF ETHICAL STANDARDS (ETİK STANDARTLARIN BEYANI)

The author of this article declares that the materials and methods they use in their work do not require ethical committee approval and/or legal-specific permission.

Bu makalenin yazarı çalışmalarında kullandıkları materyal ve yöntemlerin etik kurul izni ve/veya yasal-özel bir izin gerektirmediğini beyan ederler.

AUTHORS' CONTRIBUTIONS (YAZARLARIN KATKILARI)

***Burcu Çiçek*:** She performed numerical analyses, the results and the writing process.

Nümerik analizleri yapmış, sonuçlarını analiz etmiş ve maklenin yazım işlemini gerçekleştirmiştir.

Emre ÜRÜN: He conducted the experiments, analyzed the results and performed the writing process.

Deneyleri yapmış, sonuçlarını analiz etmiş ve maklenin yazım işlemini gerçekleştirmiştir.

Necmettin ŞAHİN: He analyzed the results and performed the writing process.

Deneysel ve nümerik sonuçları değerlendirmiş ve makalenin yazım işlemini gerçekleştirmiştir.

CONFLICT OF INTEREST (ÇIKAR ÇATIŞMASI)

There is no conflict of interest in this study.

Bu çalışmada herhangi bir çıkar çatışması yoktur

REFERENCES (KAYNAKLAR)

[1] Hamida M.B.B., Almeshaal M.A., Hajlaoui K., Rothan Y.A., A Three-Dimensional Thermal Management Study for Cooling a Square Light Edding Diode, Case Studies In Thermal Engineering, 27 (2021) 101223.

[2] Hamida M.B.B., Charrada K., Three Dimensional Dynamic Study Of a Metal Halide Thallium Iodine Discharge Plasma Powered by a Sinusoidal and Square Signal, The European Physical Journal D, 70 (2016), 1-8.

[3] Araoud Z., Ben-Ahmed R., Ben-Hamida M.B., Franke S., Stambouli M., Charrada K., Zissis G., A Two- Dimensional Modeling of the Warm-Up Phase of a High-Pressure Mercury Discharge Lamp, Physics Of Plasmas, 17(6)(2010) 063505.

[4] Zhang K., Li M.J., Wang F.L., He Y.L., Experimental and Numerical Investigation of Natural Convection Heat Transfer of W-Type Fin Arrays, International Journal Of Heat And Mass Transfer, 152 (2020) 119315.

[5] Wang J., Zhao X.J., Cai Y.X., Zhang C., Bao W.W., RETRACTED: Experimental Study on the Thermal Management of High-Power LED Headlight Cooling Device Integrated with Thermoelectric Cooler Package, (2015) 532-540.

[6] Yang K.S., Chung C.H., Tu C.W., Wong C.C., Yang T.Y., Lee M.T., Thermal Spreading Resistance Characteristics of a High Power Light Emitting Diode Module, Applied Thermal Engineering, 70(1)(2014) , 361-368.

[7] Shen L., Tu Z., Hu Q., Tao C., Chen H.,The Optimization Design and Parametric Study of Thermoelectric Radiant Cooling and Heating Panel, Applied Thermal Engineering, 112 (2017) 688-697.

[8] Jang D., Yu S.H., Lee K.S., Multidisciplinary Optimization of a Pin-Fin Radial Heat Sink for LED Lighting Applications, International Journal of Heat and Mass Transfer, 55(4) (2012), 515-521.

[9] Costa V.A., Lopes A.M., Improved Radial Heat Sink for Led Lamp Cooling, Applied Thermal Engineering, 70(1) (2014) 131-138.

[10] Hoelen C., Borel H., de Graaf J., Keuper M., Lankhorst M., Mutter C., Wegh R., Remote Phosphor LED Modules for General Illumination: Toward 200 Lm/W General Lighting LED Light Sources, In Eighth International Conference On Solid State Lighting, International Society for Optics and Photonics, (2008) 7058.

[11] Huang B.J., Tang C.W., Wu M.S., System Dynamics Model of High-Power LED Luminaire, Applied Thermal Engineering, 29(4) (2009) 609-616.

[12] Jang D., Yook S.J., Lee K.S., Optimum Design of a Radial Heat Sink with a Fin-Height Profile for High- Power LED Lighting Applications, Applied Energy, 116 (2014) 260-268.

[13] Schmid G., Valladares-Rendón L.G., Yang T.H., Chen, S.L., Numerical Analysis of the Effect of a Central Cylindrical Opening on the Heat Transfer of Radial Heat Sinks for Different Orientations, Applied Thermal Engineering, 125 (2017) 575-583.

[14] Shen Q., Sun D., Xu Y., Jin T., Zhao X., Orientation Effects on Natural Convection Heat Dissipation of Rectangular Fin Heat Sinks Mounted on Led's, International Journal of Heat and Mass Transfer, 75 (2014) 462-469.

[15] Yin L., Yang L., Yang W., Guo Y., Ma K., Li S., Zhang J., Thermal Design and Analysis of Multi-Chip LED Module with Ceramic Substrate, Solid-State Electronics, 54(12) (2010), 1520-1524.

[16] Ha M., Graham S., Development of a Thermal Resistance Model for Chip-On-Board Packaging of High Power LED Arrays, Microelectronics Reliability, 52(5) (2012) 836-844.

[17] Tang Y., Liu D., Yang H., Yang P., Thermal Effects on LED Lamp with Different Thermal Interface Materials, IEEE Transactions on Electron Devices, 63(12) (2016) 4819-4824.

[18] Abdelmlek K.B., Araoud Z., Ghnay R., Abderrazak K., Charrada K., Zissis, G., Effect of Thermal Conduction Path Deficiency on Thermal Properties of Leds Package, Applied Thermal Engineering. 102 (2016) 251-260.

[19] Moon S.H., Park Y.W., Yang H.M., A Single Unit Cooling Fins Aluminum Flat Heat Pipe for 100 W Socket Type COB LED Lamp, Applied Thermal Engineering. 126 (2016) 1164-1169.

[20] Sosoi G., Vizitiu Ş.R., Burlacu A., Galatanu C.D., A Heat pipe Cooler for High Power LED's Cooling in Harsh Conditions, Procedia Manufacturing, 32 (2017) 513-519.

[21] Joshi T., Parkash O., Krishan G., Numerical Investigation of Slurry Pressure Drop at Different Pipe Roughness in a Straight Pipe Using CFD, Arabian Journal for Science and Engineering, 47 (12) (2022), 15391-15414.

[22] Çiftçi E., AlN/Saf Su Nanoakışkanının Isı Borusu Performans Parametreleri Üzerindeki Etkilerinin Deneysel Olarak Araştırılması, Gazi University Journal of Science Part C: Design and Technology, 8(4) (2020), 858-871.

[23] Huang D.S., Chen T.C., Tsai L.T., Lin M.T., Design of Fins with a Grooved Heat Pipe for Dissipation of Heat from High Powered Automotive LED Headlights, Energy Conversion and Management, 180 (2019) 550–558.

[24] Wang H., Qu J., Peng Y., Sun Q., Heat Transfer Performance of a Novel Tubular Oscillating Heat Pipe with Sintered Copper Particles Inside Flat-Plate Evaporator and High-Power LED Heat Sink Application, Energy Conversion and Management, 189 (2019) 215–222.

[25] Lu X., Hua T-C., Wang Y.P., Thermal Analysis of High Power LED Package with HPHS, Microelectronics Journal, 42 (2011) 1257–1262.

[26] Tang Y., Luo Y., Ou P., Wang H., Ma H., Qin Y., Bai P., Zhou G., Experimental Investigation on Active Heat Sink with Heat Pipe Assistance for High-Power Automotive LED Headlights, Case Studies In Thermal Engineering, 28 (2021) 101503.

[27] Kline S.J., (1985), The Purposes of Uncertainty Analysis, Journal of Fluids Engineerings. 107, 153–160.

[28] Moffat R.J, Describing the Uncertainties in Experimental Results, Exp. Therm Fluid Sci. 1 (1) (1988) 3–17

[29] Fatchurrohman N., Chia S.T., Performance of Hybrid Nano-Micro Reinforced Mg Metal Matrix Composites Brake Calliper: Simulation Approach, In IOP Conference Series: Materials Science and Engineering, IOP Publishing. 257(1) (2017) 12060.

[30] ANSYS FLUENT Theory Guide (Release 13.0), Multiphase Flows. ANSYS, Inc. (chapter 17), (2010) 455-568.

[31] ANSYS FLUENT Theory Guide (Release 12.0), Multiphase Flows. ANSYS, Inc. (chapter 6.2.2), (2009).

[32] De Schepper S.C., Heynderickx G.J., Marin G.B., Modeling the Evaporation of a Hydrocarbon Feedstock in the Convection Section of a Steam Cracker. Computers & Chemical Engineering, 33(1) (2009) 122-132.

[33] Rammohan A., Chandramohan, V.P., Experimental Analysis on Estimating Junction Temperature and Service Life of High Power LED Array Microelectronics Reliability, 120 (2021) 114121.

[34] DS115 LUXEON COB Core Range Product Datasheet, https://www.lumileds.com/uploads/419/DS115-pdf:

[35] Zhang P., Zeng J., Chen X., Cai M., Xiao J., Yang D., An Experimental Investigation of a 100-W High-Power Light-Emitting Diode Array Using Vapor Chamber–Based Plate, Advances in Mechanical Engineering, 7(11) (2015) 1687814015620074.

[36] Lu X.Y., Hua T.C., Liu M. J., Cheng Y.X., Thermal Analysis of Loop Heat Pipe Used for High-Power LED.,Thermochimica Acta, 493(1-2) (2009) 25-29.

[37] Gwinn J.P., Webb R.L., Performance and Testing Of Thermal Interface Materials, Microelectronics Journal, 34 (3) (2003) 215-222.